A DISCRETE NUMERICAL MODEL FOR STUDYING MICRO-MECHANICAL RELATIONSHIP IN GRANULAR ASSEMBLIES

Training Report Submitted

In Partial Fulfilment of the Requirements

for the Course of

CE-390

by

Shivam Gupta
Y3331

to the

Department of Civil Engineering
INDIAN INSTITUTE OF TECHNOLOGY KANPUR

August, 2006

ABSTRACT

The discrete element method is a numerical model capable of describing the mechanical behavior of assemblies of spheres. The method is based on the use of numerical schemes in which the interaction of the particles is monitored contact by contact and the motion of the particles modeled particle by particle. In the work presented here, DEM simulations are carried out on two kinds of granular assemblies composed of randomly packed poly-dispersed grains, one with dense packing and another with loose packing. A tri-axial test is performed on these two assemblies and the results for the two are compared. With the help of Dirichlet Tessellation, neighbors are defined for each grain. All neighbors are classified among two categories: Neighbors in contact, and Neighbors without contact. The microscopic behavior is studied with the help of kinematic parameters like grain to grain displacements in which different displacements like normal displacement and tangential displacements(which include rolling, sliding) have been quantified separately. The main focus of this paper is to analyze displacement patterns of particles, specifically the particles in contact and try to deduce their behavior in terms of global parameters. The work also checks for affine hypothesis, which relates microscopic displacements taking in place of granular assembly with the strain increment imposed during the tri-axial test.

ACKNOWLEDGEMENT

I consider myself extremely fortunate for getting the opportunity to learn and work under the supervision of my training supervisors Dr. Felix Darve and Dr. Bruno Chareyre. I have no words to explain their gratefulness, constant encouragement, and active participation in carrying out this work. This work is an outcome more of their foresightedness and help rather than my own effort.

I warmly acknowledge the inspiring discussion and invaluable suggestions extended to me by Dr. B Combou in a presentation given to him explaining the delicacies involved in the subject.

I express my gratitude to Dr. Animesh Das to devote his valuable time in coordinating the internship programme making it flexible enough to optimize student benefits.

TABLE OF CONTENTS

1. Introduction……
2. Discrete Element Modeling of Granular Assemblies
   2.1 The Discrete Element Method
   2.2 Random Positioning Of Spheres
   2.3 First Compaction
   2.4 Second Compaction
   2.5 Compression
3. Analysis Of Results Obtained
   3.1 Stress Strain Curve
   3.2 Contact And Neighbors Distribution
   3.3 Normal And Tangential Displacements Of Particles
   3.4 Effect Of Size Of Increment
4 Comparison With A Theoretical Localization Hypothesis
5 Hypothesis Proposed Regarding Displacements
6 Summary And Conclusions

LIST OF FIGURES AND TABLES

LIST OF FIGURES

1. Schematic Diagram of micro-structural analysis

2.1. Calculation Cycle

2.2. Random Positioning of Spheres

2.3. Stresses acting on tri-axial test

3.1. Stress Strain Curve

3.2. Dirichlet Tessellation and Delaunay Network

3.3. Definition of filtered distance

3.4. Contact distribution for dense and loose samples

3.5. Contact coordination number and contact anisotropy

3.6. Neighbor distribution for dense and loose samples

3.7. Neighbor coordination number and neighbor anisotropy

3.8. Definition of directions for displacements

3.9 Displacement of All Neighbors with different orientations

3.10. Displacement of neighbors without contact

3.11. Displacement distribution curves for different kind of neighbors

3.12. Effect of size of increment in elastic domain

3.13. Effect of size of increment in plastic domain

4.1. Comparison between affine approximation and DEM simulations

4.2. Polar plots for comparison between affine approximation and DEM simulations

5.1. Comparison of normal displacements

5.2. Fitting normal and axial displacement curves

LIST OF TABLES

5.1. Coefficient for dense sample

5.2. Coefficient for loose sample

1. INTRODUCTION

A granular medium is composed of distinct particles which displace independently from one another and interact only at contact points. The discrete character of the medium results in a complex behavior. Characterization of the behavior is highly extensive and faces extraordinary diversity.

The final goal of the mechanics of granular materials is to provide relationships between the external loads acting on the material and the resulting displacements. Traditionally, the effect of external loads is expressed by the continuum-mechanical state variable stress, deformations are reflected by the other continuum-mechanical state variable strain. Stress and strain are related to each other through the constitutive equations(which are expected to contain all the information about the mechanical characteristics of the material).The geometrical and equilibrium equations are clear in continuum mechanics, but to find the proper constitutive equations for granular assemblies is not simple.

Recently there are two approaches: one is continuum-mechanical approach and another is micro-structural approach.

The idea of the continuum-mechanical approach is to consider the assembly as a continuous domain, taking an infinitesimal small representative volume element, and applying stress and strain as the fundamental variables that uniquely determine the state of the material at any point.

The aim of the micro-structural approach is to find macro-level state variables that are based on micro-variables such as contact forces, grain displacements, and local geometrical characteristics. In this approach the relationships between its state variables would be more strongly connected to the phenomenon taking place in the microstructure. Figure1 describes the different variables that have to be analyzed and the links which have to be established between them.

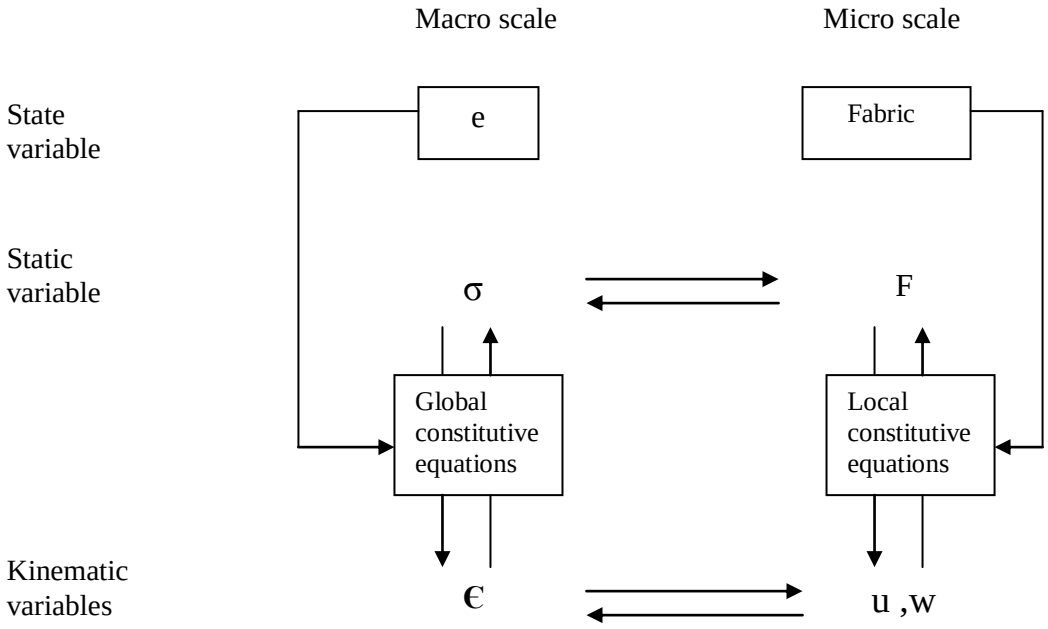

Figure1. Schematic diagram of a micro-structural analysis

To challenge the extraordinary diversified behavior of granular assemblies, discrete element method proves handy in making the prototype structures prior to the production run – "Civil Engineering has generally got to work first time."

2. DISCRETE ELEMENT MODELLLING OF GRANULAR ASSEMBLIES

2.1 The Discrete Element Method

A general particle flow model, PFC-3D simulates the mechanical behavior of a system comprised of a collection of arbitrarily shaped particles (particle here is taken as a body which takes some space, unlike the assumption of point particle taken in the field of mechanics). The model is composed of distinct particles that displace independently of one another and interact at contacts. If the particles are assumed to be rigid, and the behavior of contacts is characterized using soft contact approach, in which the rigid particles are allowed to overlap and a finite normal stiffness is taken to represent the measurable stiffness that exists at a contact, then the mechanical behavior of such a system is described in terms of the movement of each particle and the inter-particle forces acting at each contact point. Newton's laws of motion provide the fundamental relationship between particle motion and the forces causing the

motion. The assumption of rigid bodies in PFC is good for packed particle assembly or granular assembly such as sand since the deformation results primarily from the opening and interlocking at interfaces and not from individual particle deformation.

The discrete element code allows finite displacements and rotations of discrete bodies, including complete detachment, and recognizes new contacts automatically as the calculation progresses. The calculation cycle in PFC-3D is a time-stepping algorithm that requires the repeated application of the laws of motion to each particle, a force displacement law to each contact, and a constant updating of wall positions. The calculation cycle is illustrated in Figure 2.1. At the start of each time-step, the set of contacts is updated from the known particle and wall positions. The force-displacement law is then applied to each contact to update the contact forces based on the relative motion between the two entities at the contact. Next, the law of motion is applied to each particle to update its velocity and position based on the resultant force and the moment arising from the contact forces acting on the particle. Also, the wall positions are updated based on the specified wall velocities.

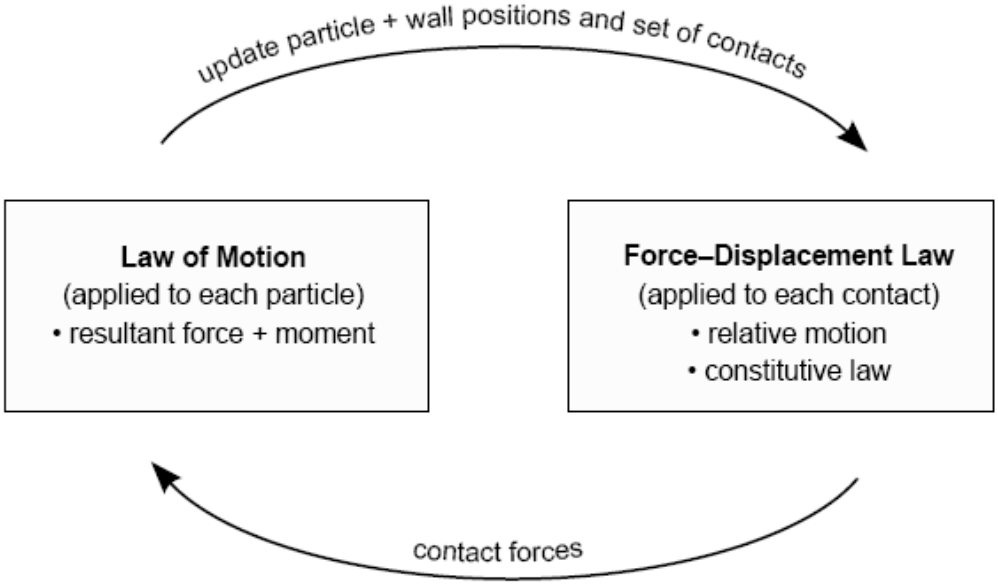

Figure 2.1 Calculation Cycle

2.2 Random Positioning Of Spheres

With the help of PFC, 4000 particles are generated having Gaussian distribution with a standard deviation of 0.33. The spheres are generated in a cell of dimensions 0.075*0.075*(1.333*0.075) m^3 in such a way that they don't have any overlap with each other and they don't touch the boundary within which they are generated. No

contact is created during this generation. The porosity of the generated is 0.33 for dense sample and 0.41 for the loose sample. Particle to particle friction coefficient is set to 0.7. Walls of the cell are taken as frictionless. The normal and tangential stiffness of contacts are set to $5*10^8$ N/m and $5*10^7$ N/m. As shown in Figure 2.2, the spheres marked cross are not accepted during this generation.

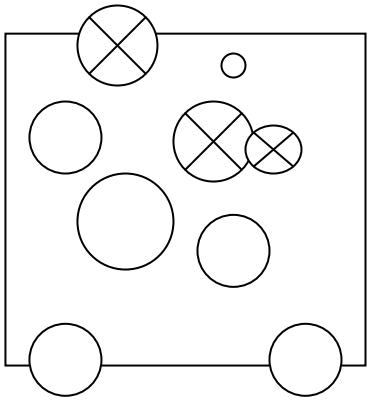

Figure 2.2 Random positioning of spheres

2.3 First Compaction

The cell generated is compacted until the mean stress in the sample becomes equal to the desired confining pressure. This is done in two steps. Firstly, the mean stress is calculated. Then a dynamic loop is run in which it is compared with the desired confining pressure. The desired isotropic confining pressure obtained is equal to 10000 N/m^2. If the mean pressure is less or more than the confining pressure required, then the radius of the grains are increased or decreased respectively by a constant factor of 1.0005.

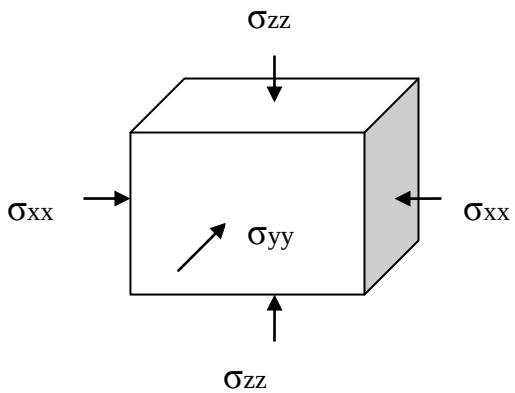

Figure 2.3 Stresses acting on tri-axial cell

$$\text{Mean Stress} = \frac{\sigma_{xx} + \sigma_{yy} + \sigma_{zz}}{3}$$

2.4 Second Compaction

Contact friction is a major parameter which helps in generating dense and loose samples. Porosity depends upon contact friction. If contact friction is high, grains don't have much tendency to move and they tend to stick with their neighbors and therefore there is less tendency of a new grain filling the void space. Whereas if the friction is low, grains will easily roll and slide and the tendency for rearrangement will be much higher and they eventually fill out the void space.

In second compaction, specifying particular contact friction, dense and loose samples are generated. The boundary walls are moved and a control is imposed so that all the stresses, σ_{xx}, σ_{yy}, σ_{zz} become equal to the confining pressure σ_o and we have an assembly with isotropic confinement.

2.5 Compression

In this step, σ_{xx} and σ_{yy} are maintained equal to the confining isotropic pressure, and the walls in the z- direction are moved with constant vertical velocity equal to 0.001.

3. ANALYSIS OF RESULTS OBTAINED

3.1 Stress Strain Curve

Figure 3.1 shows the evolution of the deviatoric stress with 4000 intermediate states obtained with the strain increments and it's comparison with the evolution of porosity.

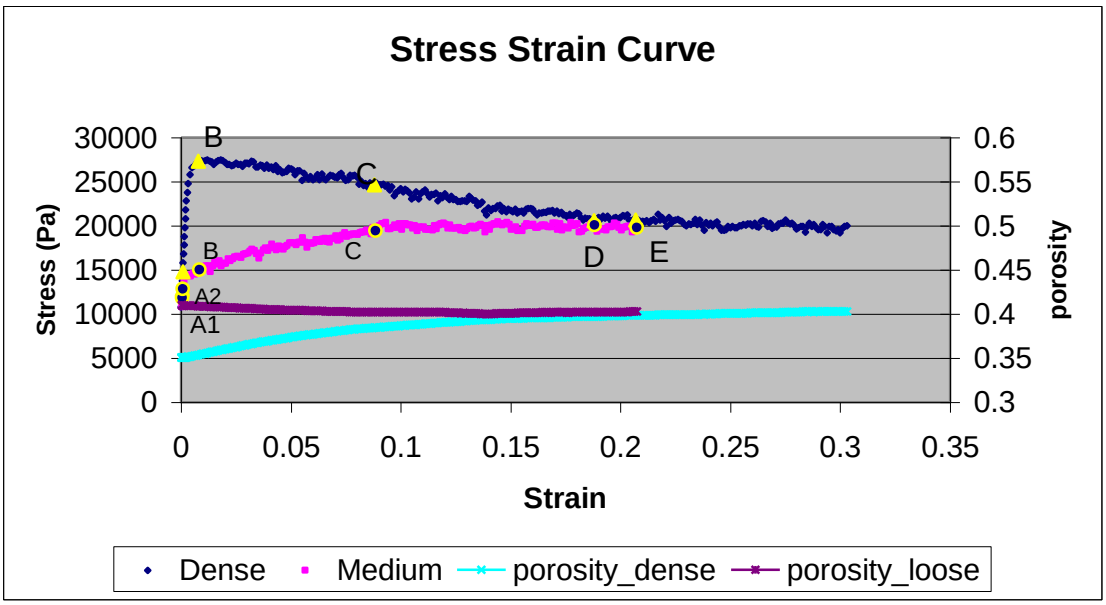

Figure3.1 Stress Strain curve

The tri-axial test is carried out on the dense and loose granular assemblies. Marks A1, A2, B, C, D, E corresponds to the points in different characteristic regions of stress strain curve.A1 and A2 correspond to elastic part, B to peak, C to strain softening, D and E to critical state in the dense sample. Points in the loose sample correspond to the same strain as its counterpart in the dense sample. In the dense sample, it behaves elastically in the beginning of the compression. But after a strain of about 0.003 there is introduction of plasticity in the sample. The sample undergoes strain hardening, it's strength increases and it's capacity to sustain high stresses. During compaction, the porosity increases, the sample dilates and signifies the strain softening of the sample. At a strain of about 0.25, stress in the sample becomes constant. This state is called critical state. The logic behind the critical state lies in the understanding which says that a sample can never be compressed or dilated indefinitely.

In the loose sample, the grains undergo rearrangement and they tend to fill out the empty void space as evident from the monotonic decreasing behavior of the porosity. Gradually, both dense and loose samples reach to same critical states with similar porosity.

3.2 Contact And Neighbor Distributions

Definition of a Neighbor

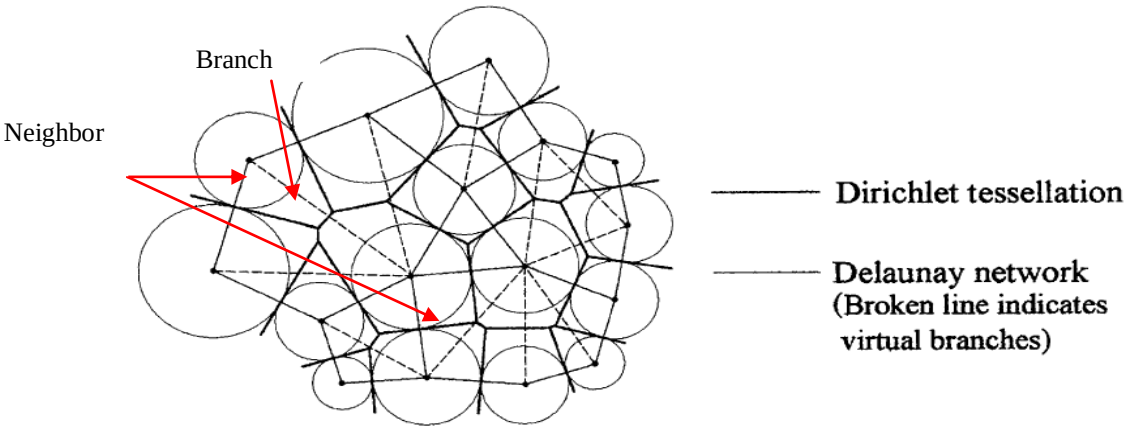

Figure3.2. Dirichlet Tessellation and Delaunay Network

The model used here employs Dirichlet Tessellation to define what is neighbor to a particle. In the assembly consisting of particles, the space is divided into domains. These domains are formed by collecting all those points which are nearer to a particle

than any other neighboring particle. There is exactly one particle in each domain. If two particles are in contact, the corresponding domains will have a common face that contains the contact point itself. These domains are referred to as material cells, and the total system given by them is called material cell system. When two material cells have a common face, the corresponding particle centers are connected by a straight line. These particles are called to be neighbors (even if there is no contact between two particles). After connecting particle centers of all such neighbors it forms a triangulation network in 2D and tetrahedron in 3D.

If we analyze all particles in tri-axial test, the results obtained for particles well inside the cell would be quite different from the behavior of particles adjacent to boundaries. To eliminate this boundary effect, we use filter distance to screen out the particles which are close enough to have a contact with the boundary. We have tried different filter distances like 0, 2 and 4 (in terms of mean radius of the particles) to observe its effect and finally fixed 2 in our analysis.

In the samples generated, of neighbors in contact, and total number of neighbors are measured as a function of orientation. In a particular orientation, these measurements are done in a cone formed by θ-dθ and θ+dθ. The result is given in terms of distribution of density of neighbors rather than actual number. Density of neighbors in a given orientation is expressed as

$$F(\theta) = \frac{N(\theta,d\theta)}{S(\theta,d\theta)}$$

where N represents number of contacts in θ-dθ and θ+dθ and S represents the area of unit sphere enveloping the same region.

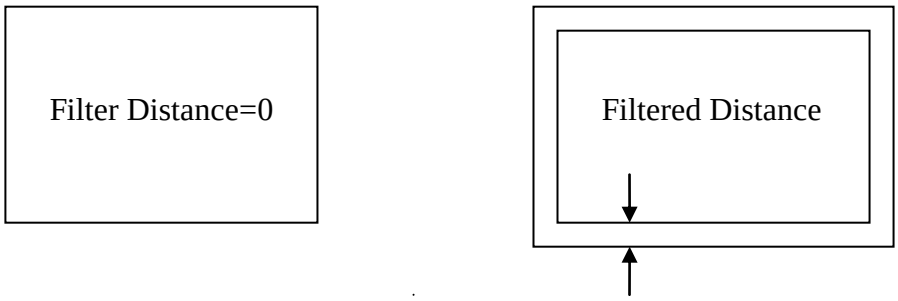

Figure3.3. Definition of Filtered Distance

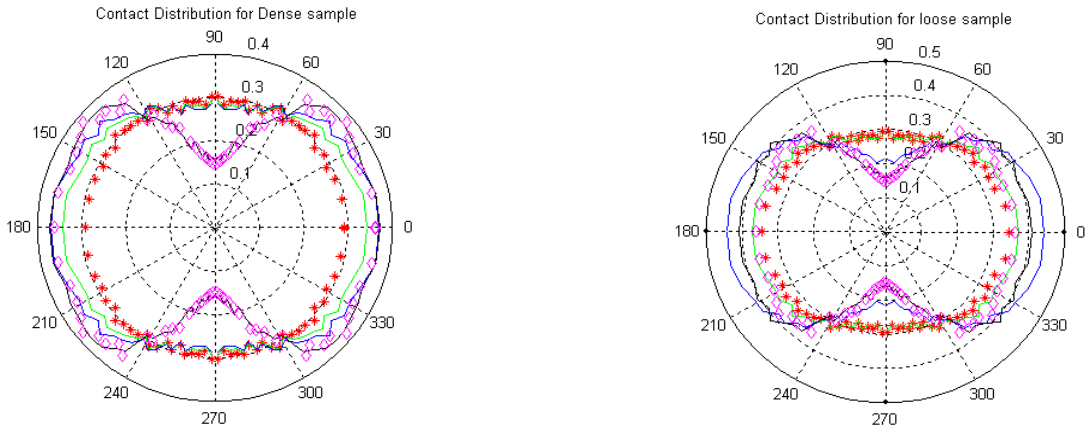

Figure3.4. Contact Distribution for dense and loose samples

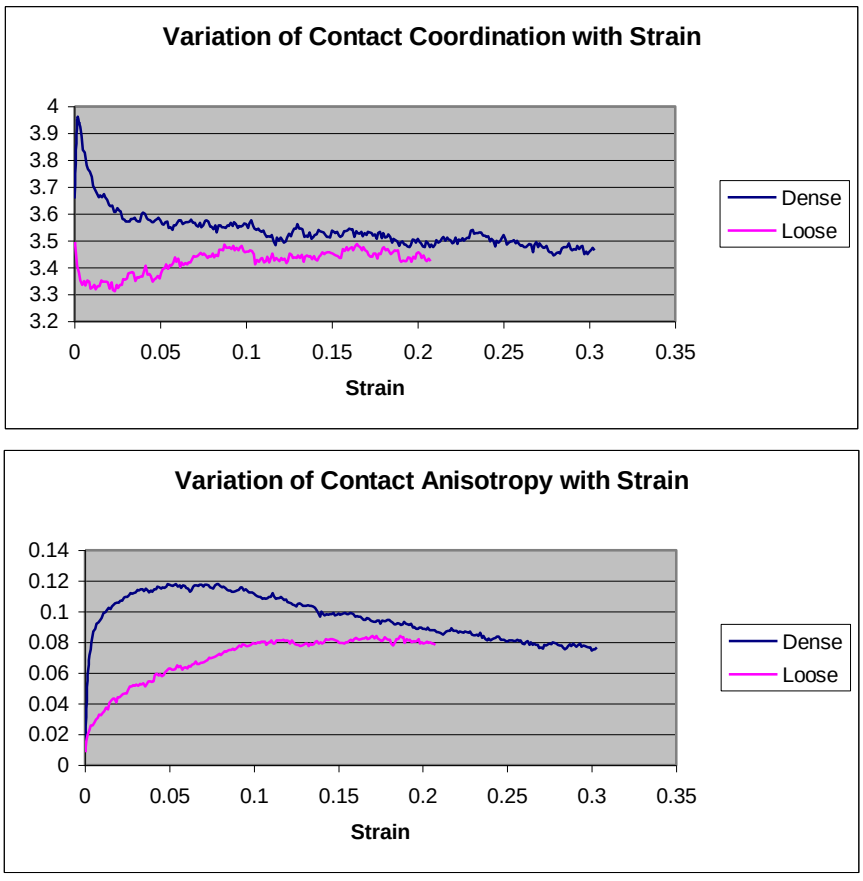

Figure 3.5.Contact Coordination and Contact Anisotropy

In the beginning of the tri-axial test, contacts are uniformly distributed throughout the sample. As compression proceeds, more and more contacts are formed in the direction of loading (θ=0°) and lost in the transverse direction (θ=90°). In dense sample, contact coordination number increases, but after some time the rate of

creation of contacts due to compression exceeds the rate of loss of contacts due to dilation and the contact coordination number starts decreasing. Whereas in loose sample, since there is lot of empty space, there is always a tendency to fill this empty space with particles and generate more and more contacts in the process. The anisotropy of both loose and dense sample is expected to increase and reach a constant value at the critical state. The decreasing behavior of anisotropy in dense sample is a matter of concern and is still in the thinking process.

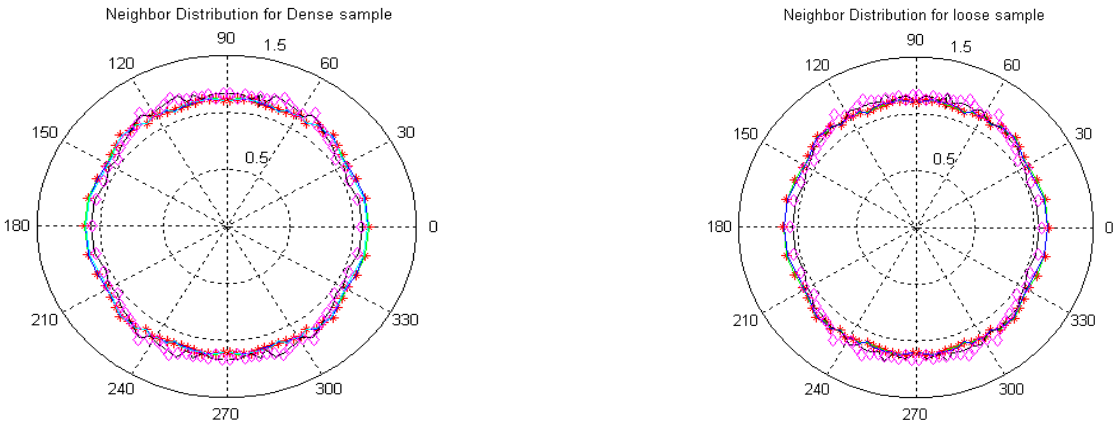

Figure3.6. Neighbor Distribution for dense and loose samples

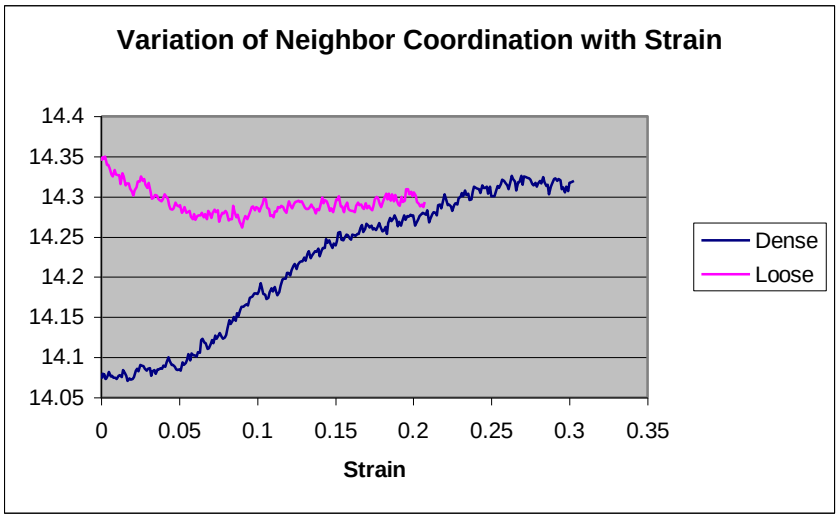

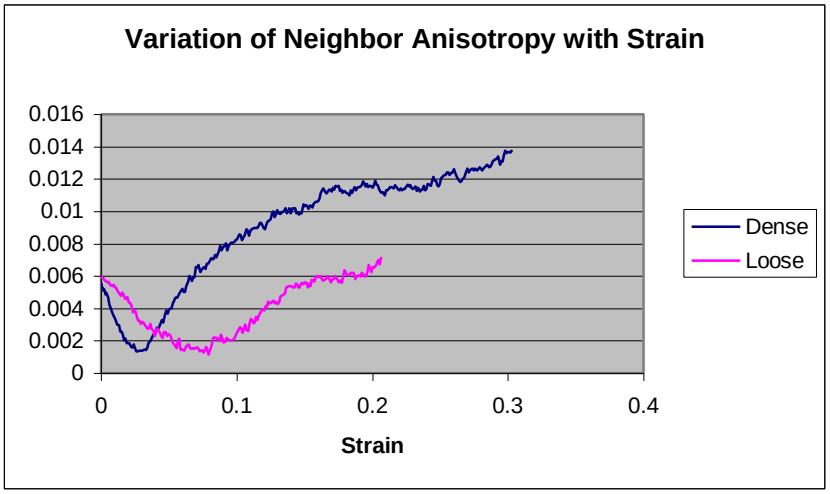

Figure 3.7.Neighbors Coordination and Neighbor Anisotropy

Neighbors Distribution remains constant throughout the tri-axial test. This can be explained by the fact that in dense assembly, the grains may rearrange among themselves but the coordination number will remain almost same. Figure 3.7 shows that the range of change of neighbor coordination number is 14.05 to 14.3 which is very small. So essentially, neighbor coordination number is constant.

3.3 Normal And Tangential Displacements Of Particles:

Figure 3.8 shows the definition of direction of normal and tangential movements. Tangential movements are broken into two components. One aligned in the plane defined by Z-Z axis and the normal, called axial tangential and another perpendicular to this plane, called transverse tangential.

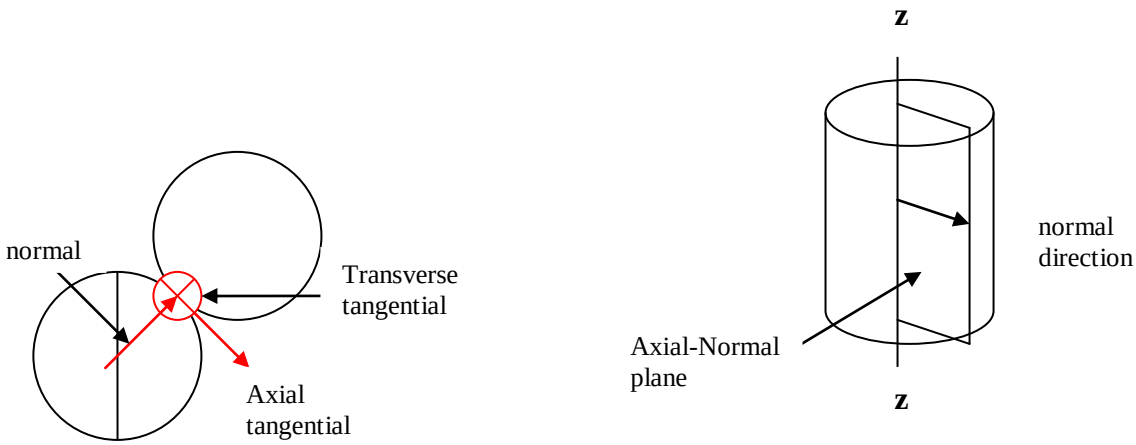

Figure 3.8.Definition of directions for displacements

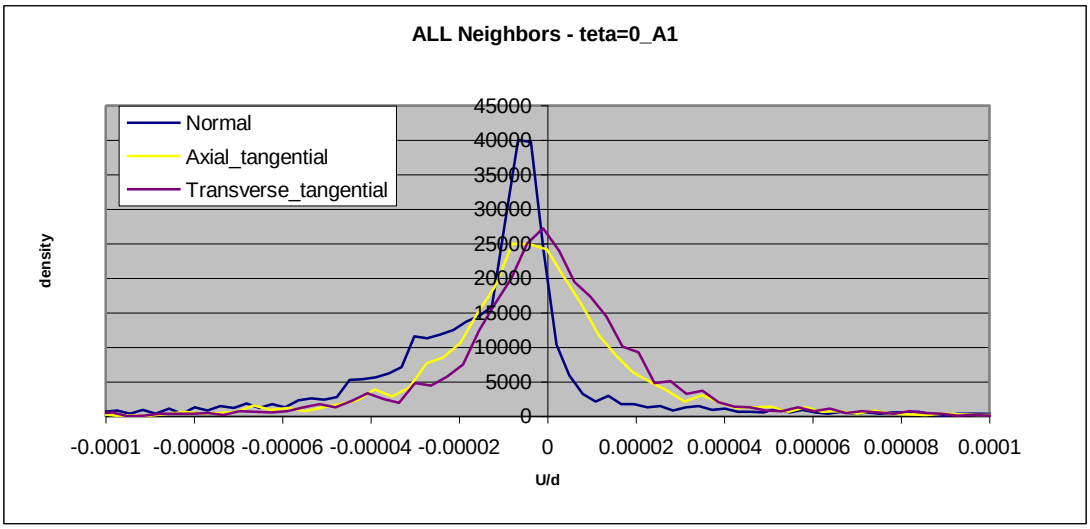

(a)

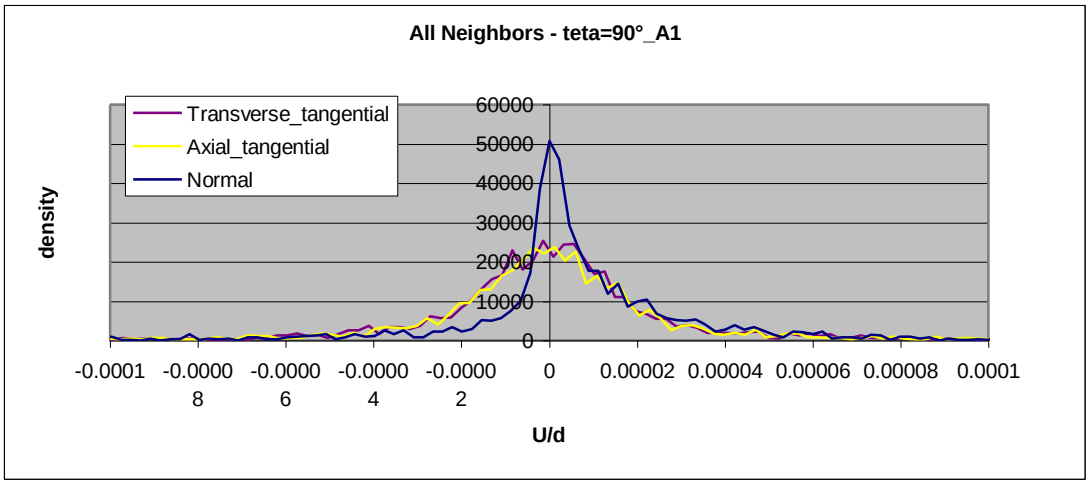

(b)

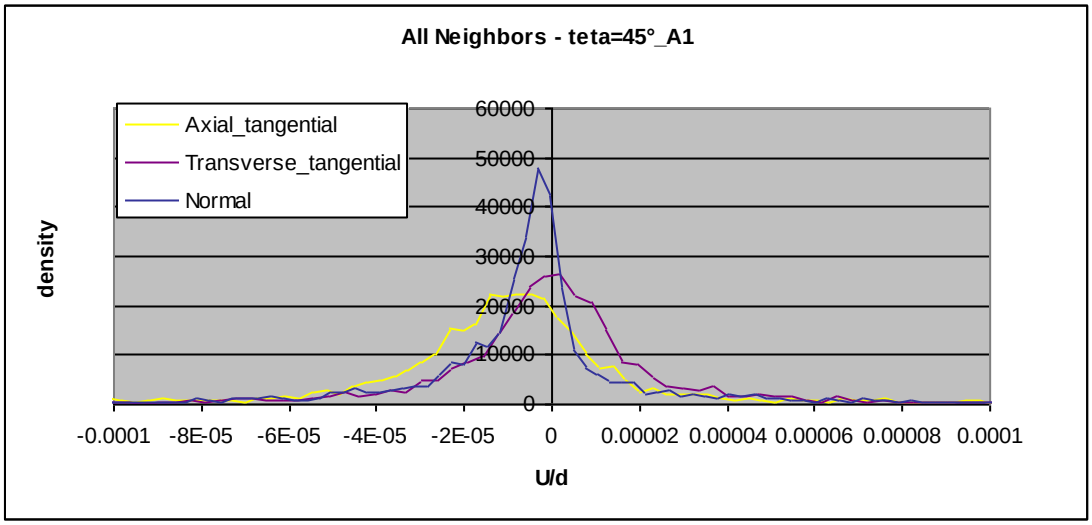

(c)

Figure 3.9.Displacements of All Neighbors with different orientations

Figure 3.9 shows normal, axial, and transverse tangential displacement of dense sample in the elastic region corresponding to strain increment A1. It has been observed that the tangential movements have more spread distribution as compared to normal displacements which are restrained by the contacts with the neighboring grains.

In orientation θ = 0°, mean of normal displacements is negative since in the direction of compression, the density of particles getting compressed is more than the particles getting dilated. In θ = 90°, mean is positive as expected. Whereas in θ = 45°, mean is negative. This can be explained by the fact that dilative movement can be calculated by employing poisson's ratio. Since poisson's ratio is less than 1, therefore the magnitude of dilation is less than compression and their resultant comes out to be negative.

The mean of the transverse tangential movements is always equal to 0, and the mean of axial tangential is equal to 0 only in the orientation 0° and 90°. This can be explained by affine hypothesis, if assumed correct, that the tangential displacements can be expressed as Uta = Є*n*t_at and Utt = Є*n*t_tt. The transverse tangential is equal to 0 because of bi-axial symmetry and in orientation 0° and 90°, the normal vector becomes an eigen vector and therefore the product Є*n is proportional to n. Since t_at is perpendicular to n, therefore its dot product comes out to be 0.

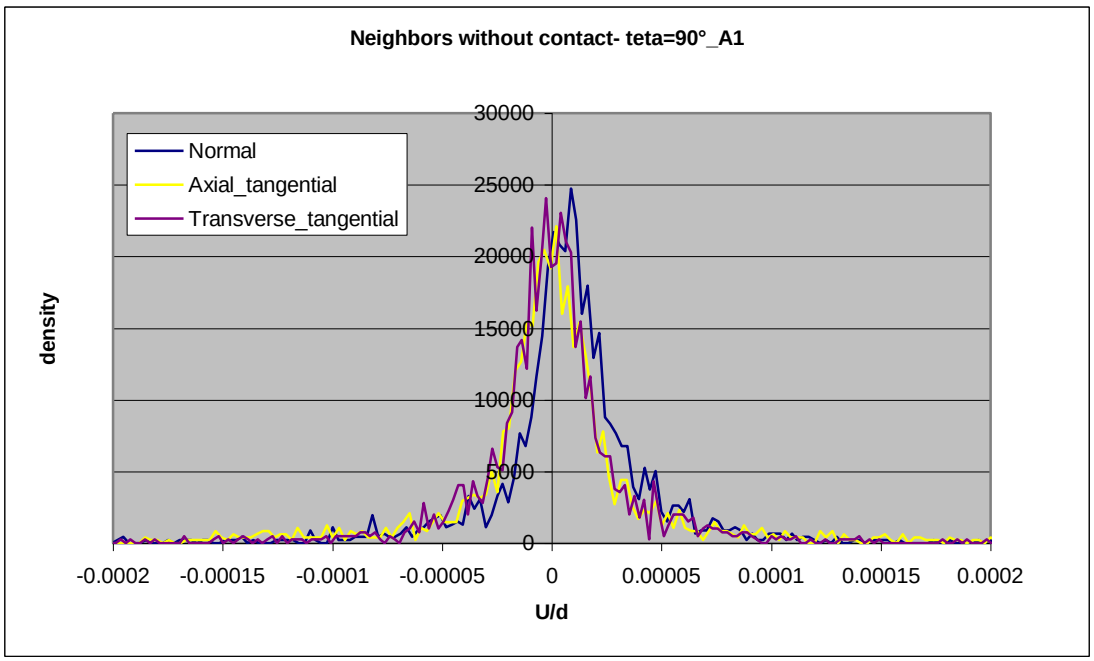

Figure 3.10.Displacement of Neighbors without contact

As shown in Figure 3.10 normal, axial tangential, transverse tangential movements distribution coincide each other because without contact, there is no contact force and a particle has equal probability to move in either of three directions.

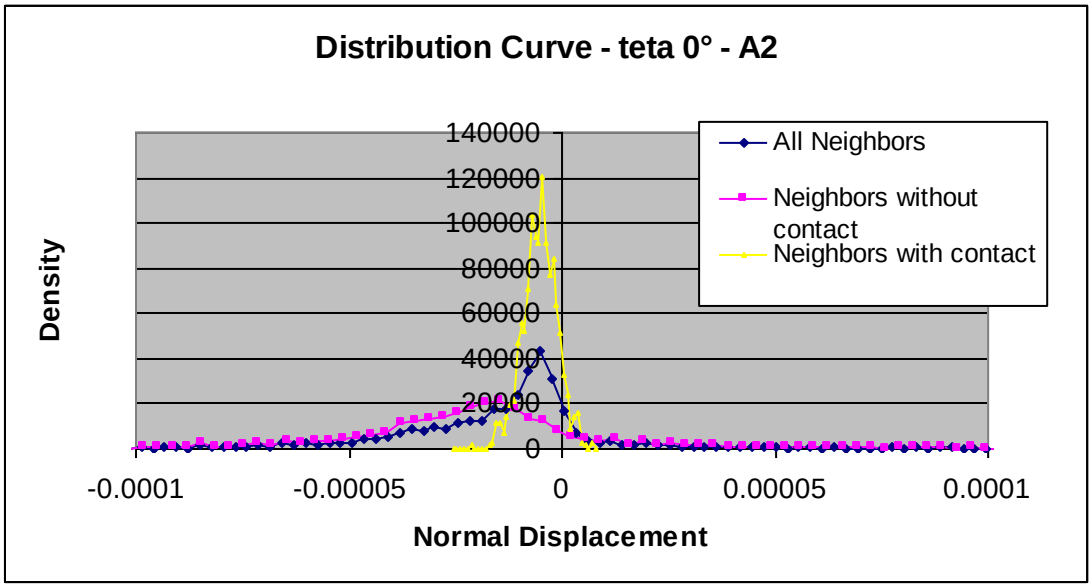

(a)

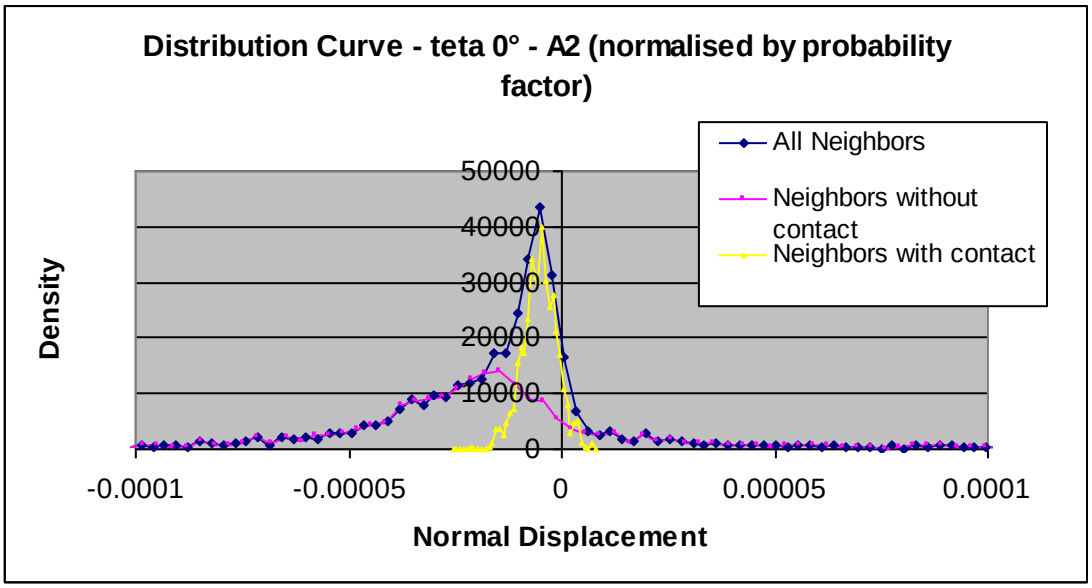

(b)

Figure 3.11.Displacement Distribution curves for different kinds of neighbors

The only difference between Figure 3.11 (a) and (b) is a probability factor. In plot (b), the distribution curves have been multiplied by the probability factor p, given by Ni/N. For all neighbors, p = 1; for neighbors without contact, p = N (without

contact)/N (all); for neighbors in contact, p = N (in contact)/N (all). This is done because the displacements of all neighbors can be given by the equation: Un (all) = p*Un (contact) + (1-p)*Un (without contact). From the plot, it is evident that in the initial stage of compaction, free movements contribute mostly for the normal displacements. After sufficient contacts are formed, the particles in contact provide most of the normal displacements.

Similar results are obtained for loose sample.

3.4 Effect Of The size Of Increment:

Size of strain increment is an important factor. Since most of the time we work with the derivatives, therefore we must choose an increment sufficiently small so that the value of the derivative is well defined. But if we choose very small increment, then results obtained will have lot of disturbance because of noise.

The effect of increment size has been looked in elastic domain and plastic domain. The domains are such that stress varies linearly with strain so that we can analyze purely elastic and purely plastic behaviors. The elastic domain is taken from state file 30 to state file 140. State file 200 corresponds to near peak. It is included mainly to see the deviation from the behavior because of introduction of plasticity. The plastic domain is taken from state file 3000 to state file 3100. The mean of transverse tangential is equal to 0 and have been excluded from this analysis.

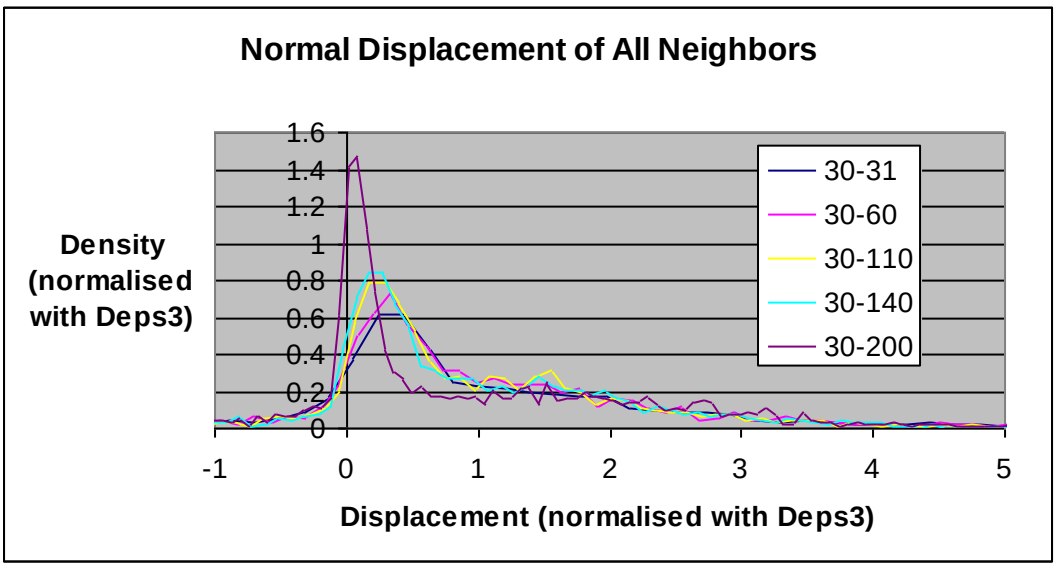

(a)

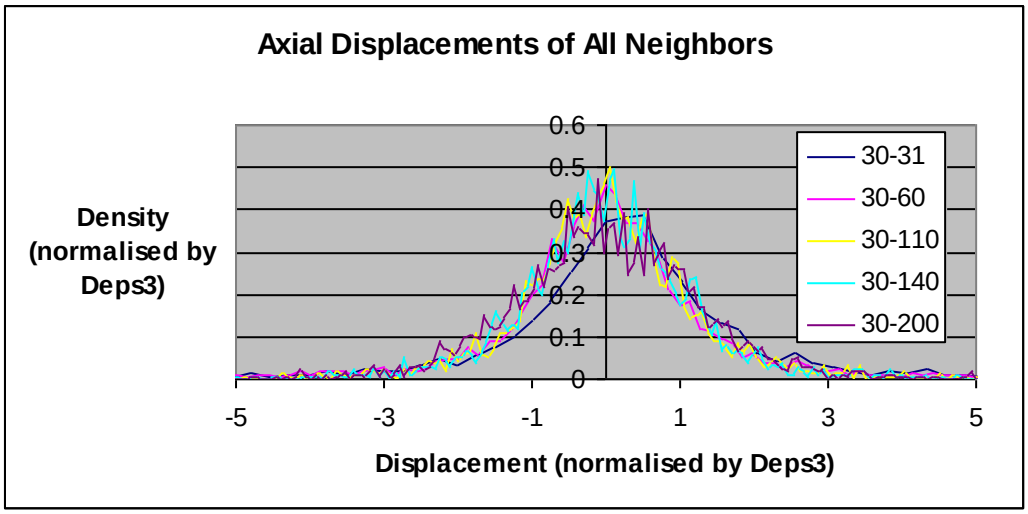
Axial Displacements of All Neighbors
Density (normalised by Deps3)
0.6
0.5
0.4
0.3
0.2
0.1
0
-5
-3
-1
1
3
5
Displacement (normalised by Deps3)
30-31
30-60
30-110
30-140
30-200

(b)

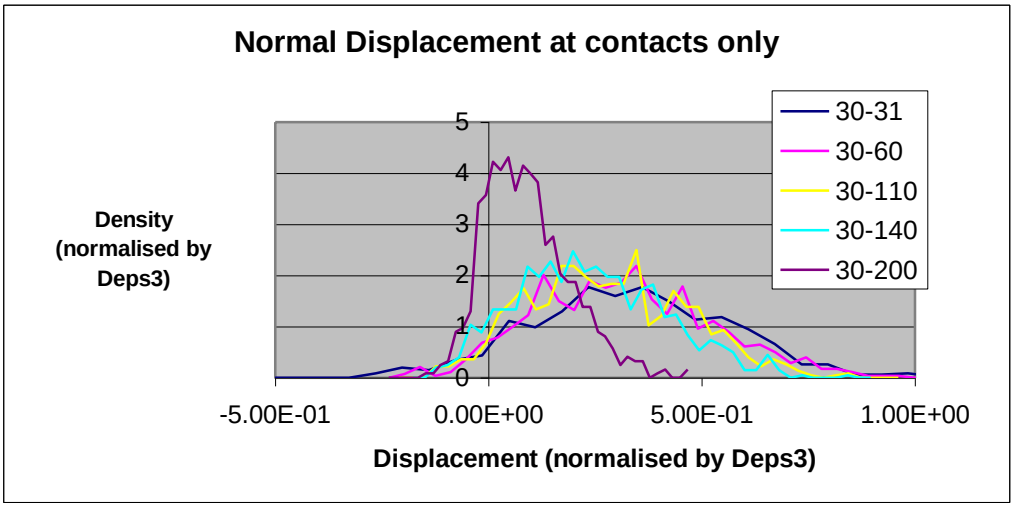
Normal Displacement at contacts only
Density (normalised by Deps3)
5
4
3
2
1
0
-5.00E-01
0.00E+00
5.00E-01
1.00E+00
Displacement (normalised by Deps3)
30-31
30-60
30-110
30-140
30-200

(c)

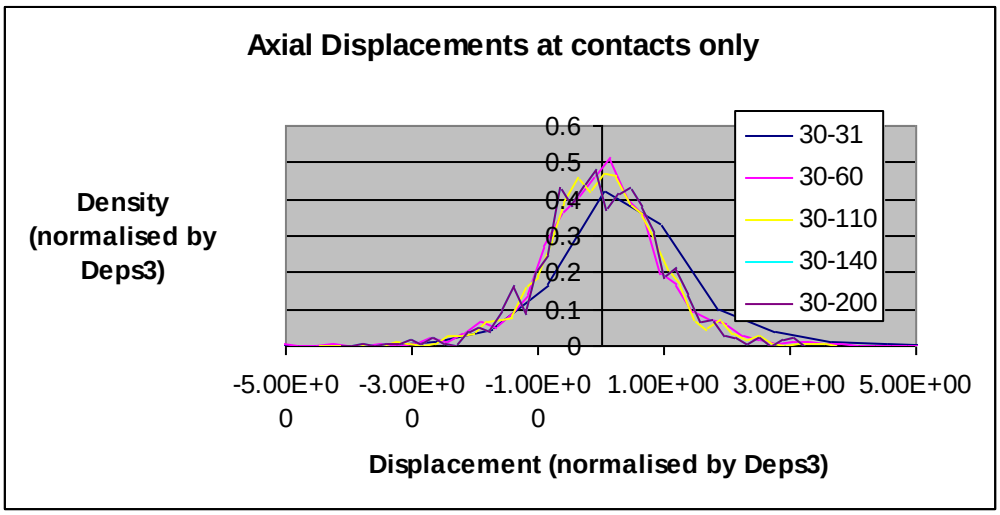
Axial Displacements at contacts only
Density (normalised by Deps3)
0.6
0.5
0.4
0.3
0.2
0.1
0
-5.00E+00
-3.00E+00
-1.00E+00
1.00E+00
3.00E+00
5.00E+00
Displacement (normalised by Deps3)
30-31
30-60
30-110
30-140
30-200

(d)

As shown in Figure 3.12 (a), (b), (c) and (d) there is no effect of the size of increment on distribution of normal and axial displacements. This means that the displacements are affected by the strain increment that is imposed during the loading only and is independent of its loading history. Figure 3.12 (e) and (f) shows that the standard deviation is linear to the size of increment.

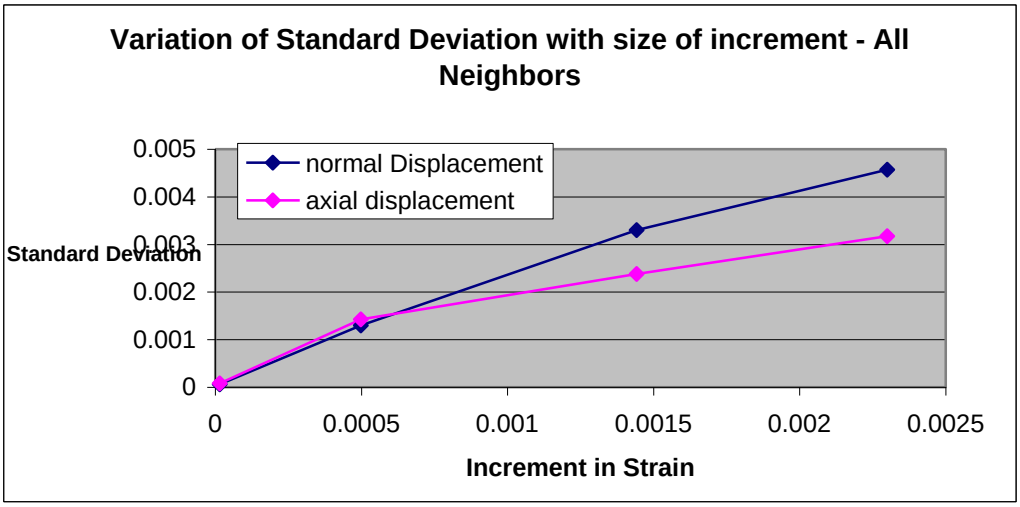

(e)

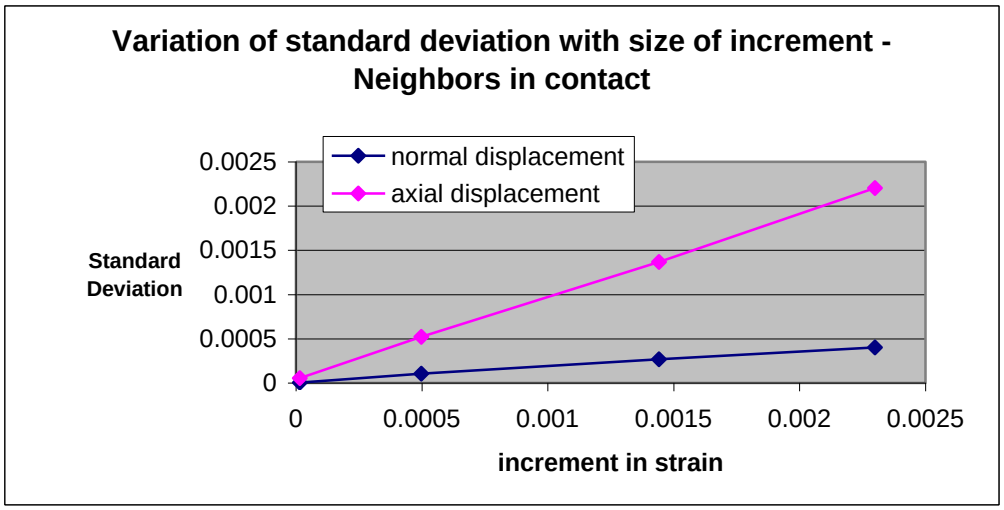

(f)

Figure 3.12.Effect of size of increment in elastic domain

From this linear behavior it can be concluded that although the assembly is composed of random particles, but when we multiply the displacement by a factor n, then the displacement field is also magnified by the same factor.

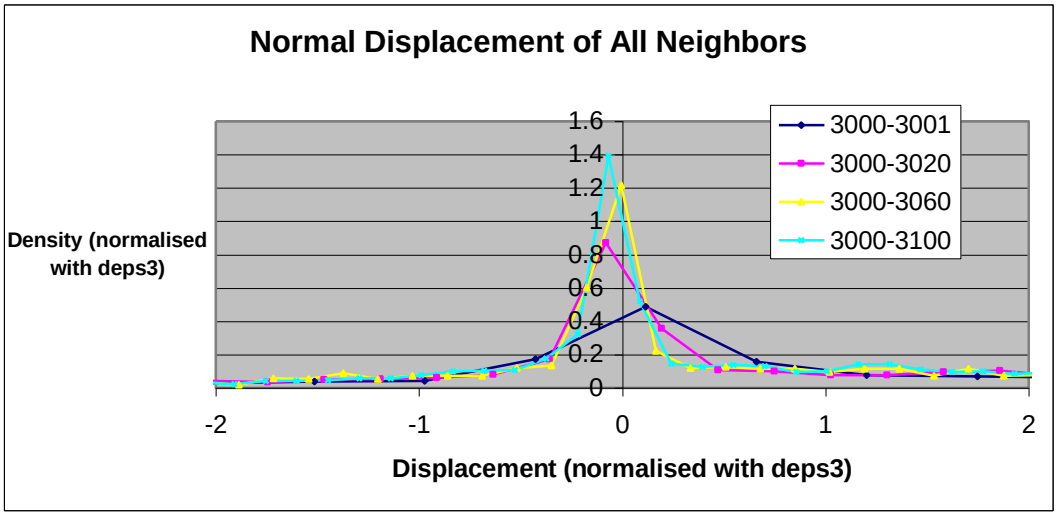
Normal Displacement of All Neighbors
Density (normalised with deps3)
1.6
1.4
1.2
1
0.8
0.6
0.4
0.2
0
-2
-1
0
1
2
Displacement (normalised with deps3)
3000-3001
3000-3020
3000-3060
3000-3100

(a)

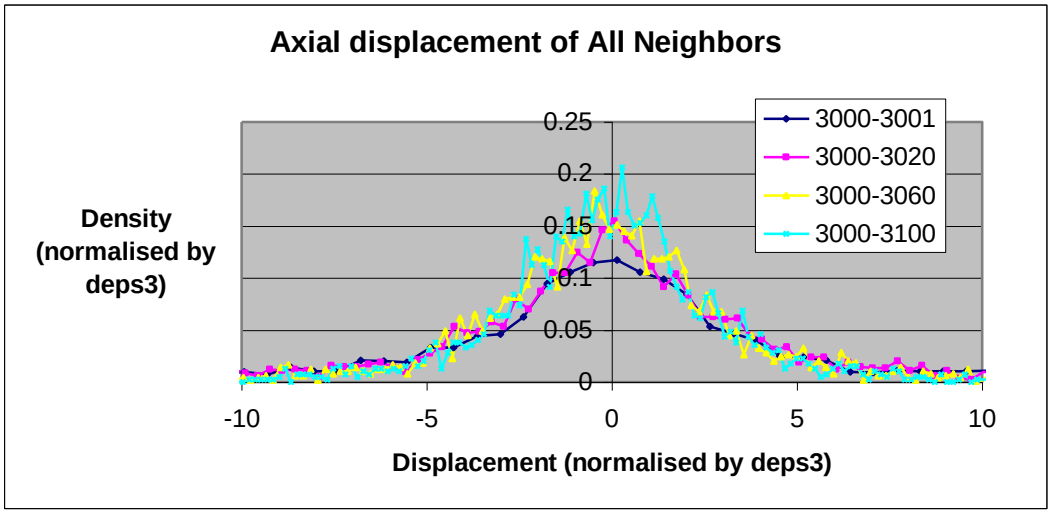
Axial displacement of All Neighbors
Density (normalised by deps3)
0.25
0.2
0.15
0.1
0.05
0
-10
-5
0
5
10
Displacement (normalised by deps3)
3000-3001
3000-3020
3000-3060
3000-3100

(b)

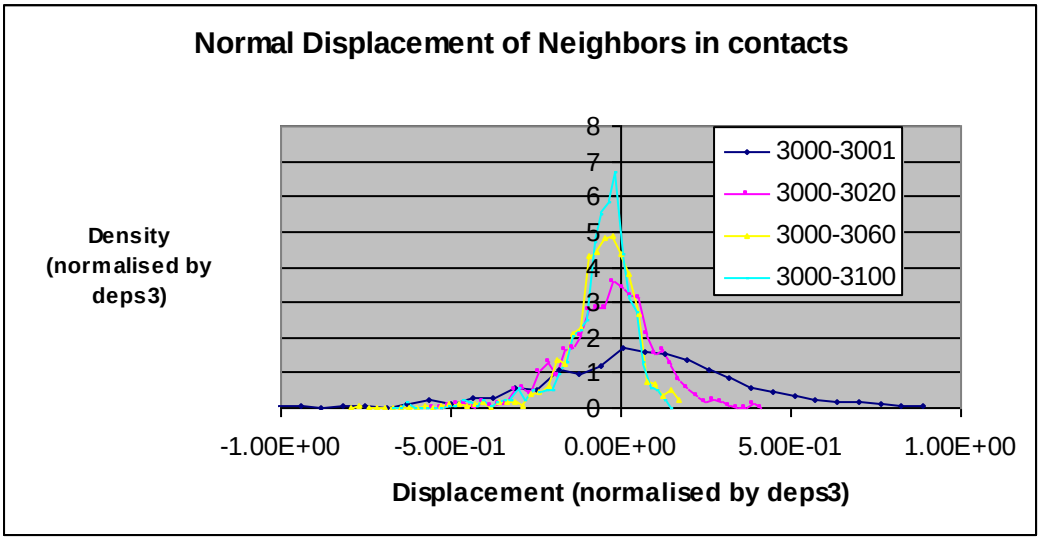
Normal Displacement of Neighbors in contacts
Density (normalised by deps3)
8
7
6
5
4
3
2
1
0
-1.00E+00
-5.00E-01
0.00E+00
5.00E-01
1.00E+00
Displacement (normalised by deps3)
3000-3001
3000-3020
3000-3060
3000-3100

(c)

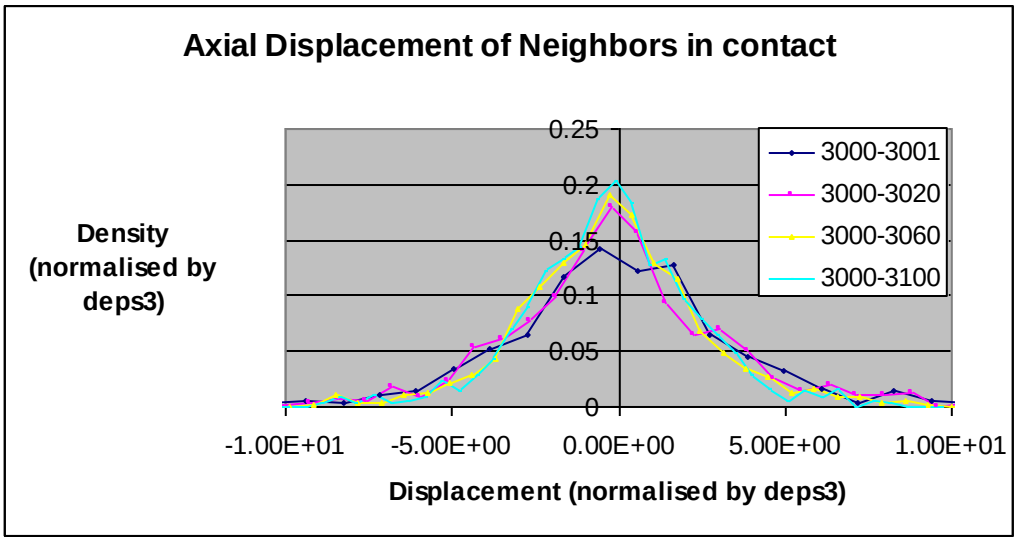

(d)

Figure 3.13 (a), (b), (c) and (d) shows the effect of increment in the plastic domain. As evident from the plots, normal displacements are affected by the size of the increment. With bigger increment, the displacement field becomes less spread. This kind of behavior is expected. In a random assembly like this, particles undergo Brownian movements where the displacement field is affected by its loading history. As in Brownian movements where the displacement field is proportional to the square root of time increment, we can see the linear variation of standard deviation with the square root of strain increment in Figure 3.13 (e) and (f).

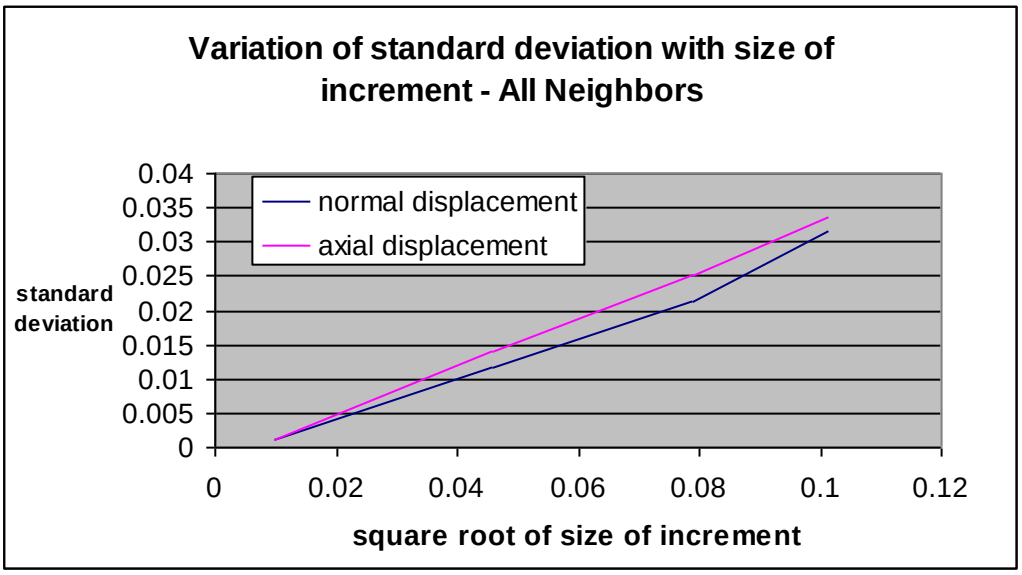

(e)

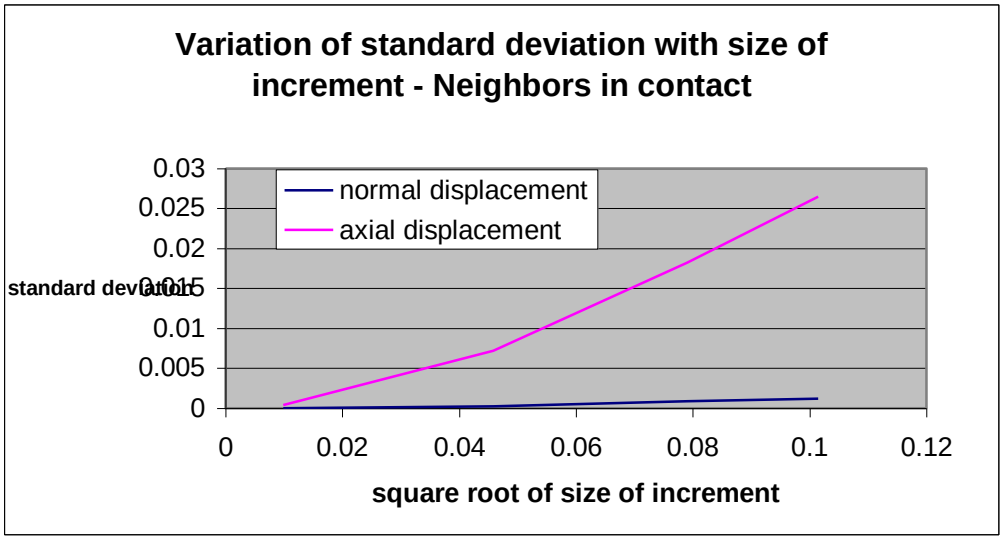

(f)

Figure 3.13 Effect of size of increment in plastic domain

4. Comparison With A Theoretical Localisation Hypothesis

Affine hypothesis comes from an analogy with the displacement of two points in an affine displacement field. It says that the displacement field generated during a tri-axial test is related to the strain by the expression U = Є.n.r where Є is the strain tensor, n is the normal vector directed towards contact, and r is a vector giving the direction of the displacement. Figure 4.2(a) shows polar plots for normal displacements of all neighbors at three points in the stress strain curve. The solid line represents points obtained using affine approximation and the dotted line with points marked represents the results obtained by numerical simulation. Figure 4.2(b), (c), (d), (e) and (f) shows similar plots for axial displacements of all neighbors; normal and axial displacements of neighbors in contact only; normal and axial displacements for neighbors without contacts. Figure 4.1 shows that transverse tangential displacements are very small as compared to normal and axial tangential displacements and hence are not of much significance.

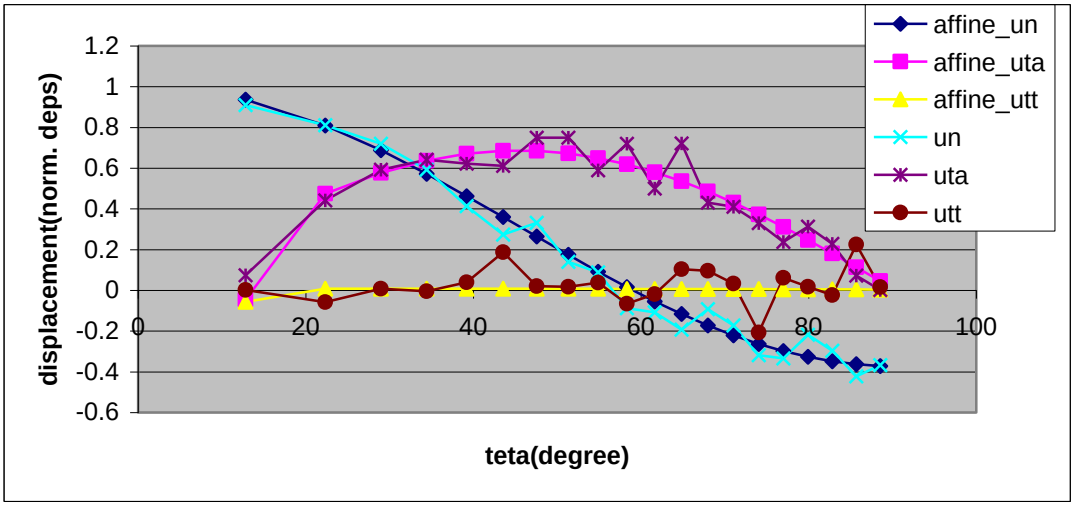

Figure 4.1 Comparison between affine approximation and DEM simulations

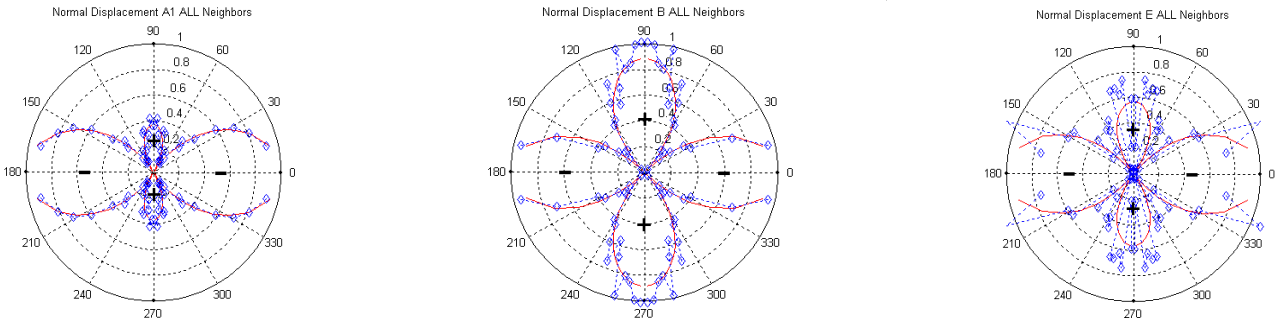

(a) Normal Displacement for All Neighbors

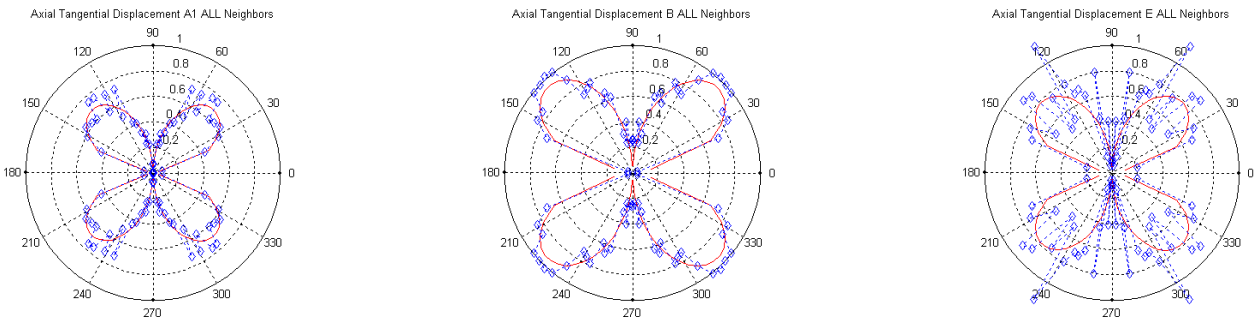

(b) Axial Displacement for All Neighbors

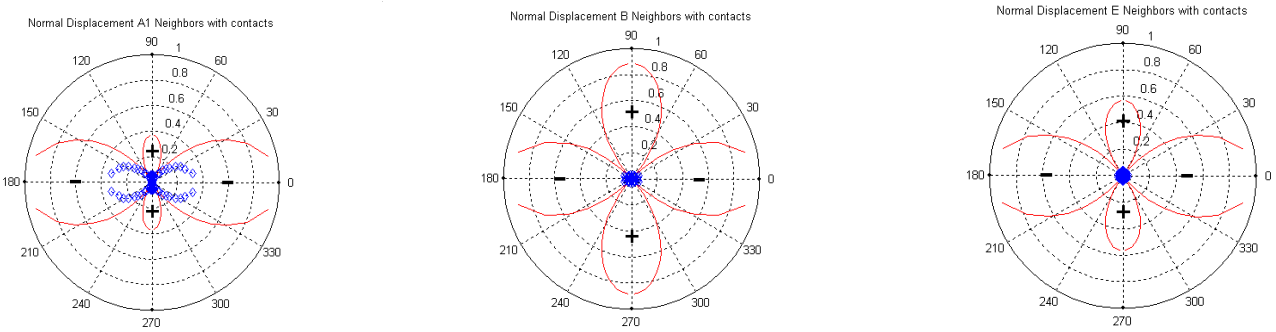

(c) Normal displacement of neighbors in contact

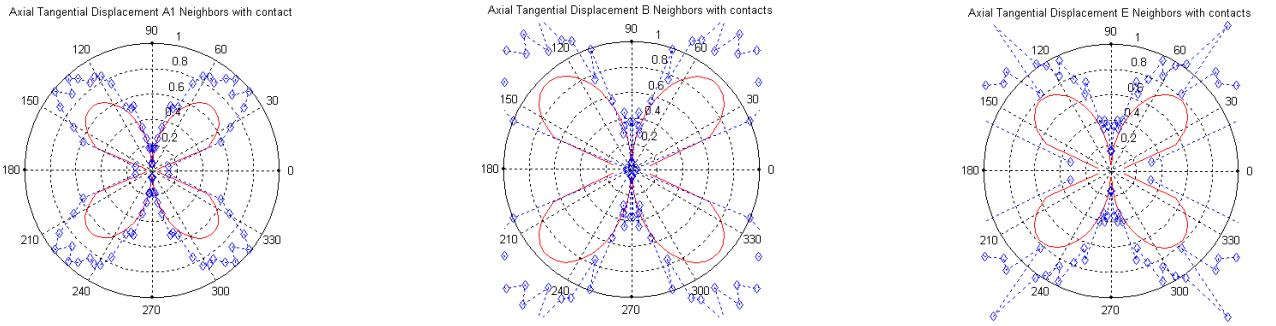

(d) Axial displacement of neighbors in contact

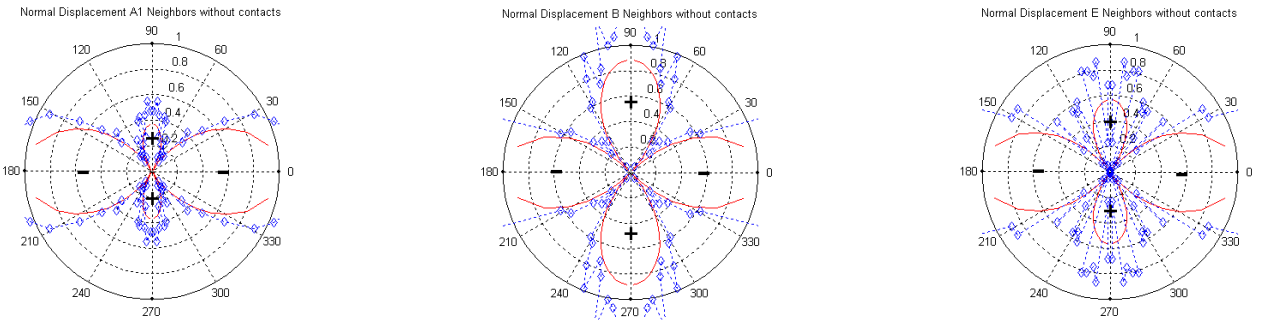

(e) Normal displacements for neighbors without contact

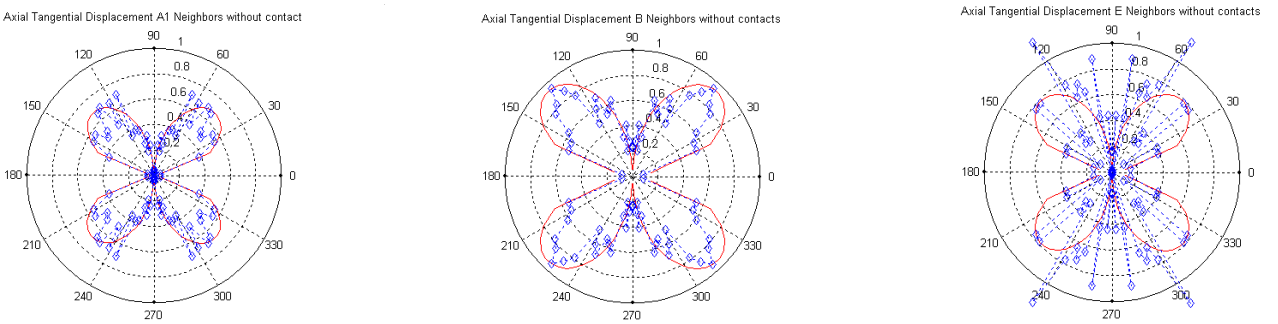

(f) Axial displacements for neighbors without contact

Figure 4.2 Polar plots for comparison between affine approximation and DEM simulation

As seen from the plots in Figure 4.2, it can be said that affine approximation holds very good for normal and axial displacements of all neighbors. It is also good displacements of neighbors without contacts also. But for neighbors with contacts, which are of main significance, affine approximation overestimates normal displacements and underestimates axial displacements. The following section tries to correlate the displacements of all neighbors and neighbors in contact.

5. Hypothesis Proposed Regarding Displacements

Displacements of contacts were compared with the affine approximation for displacements of all neighbors. Figure 5.1 shows the plots of normal displacements of all neighbors and neighbors in contact. It looks like there exist linear relationship between two displacements since there are always two constant factors relating them.

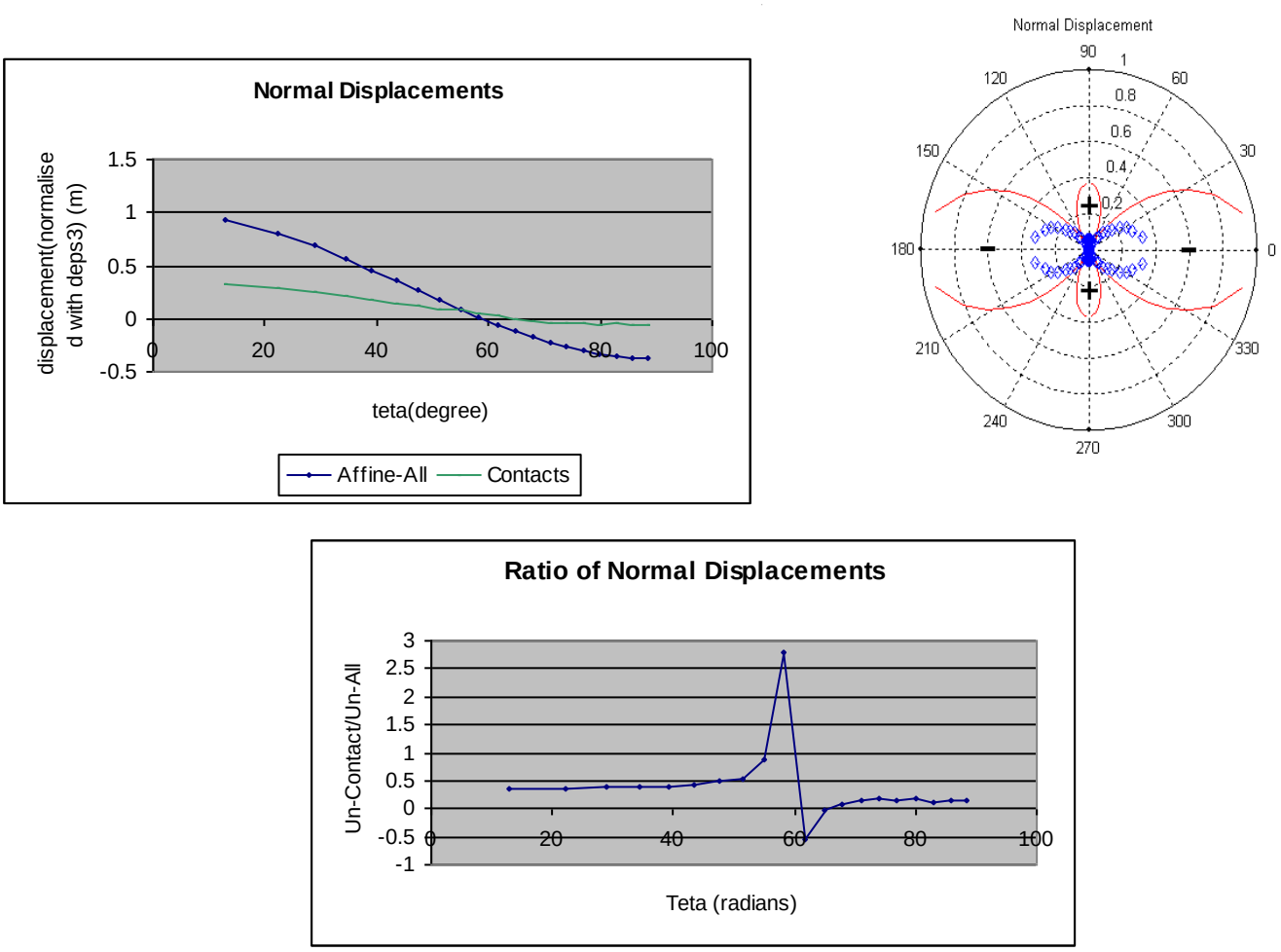

Figure 5.1 Comparison of normal displacements

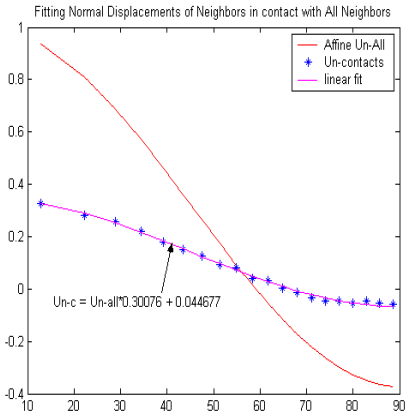

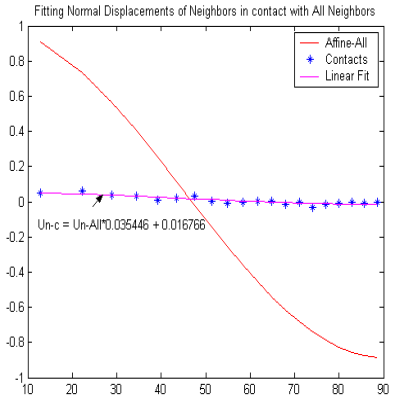

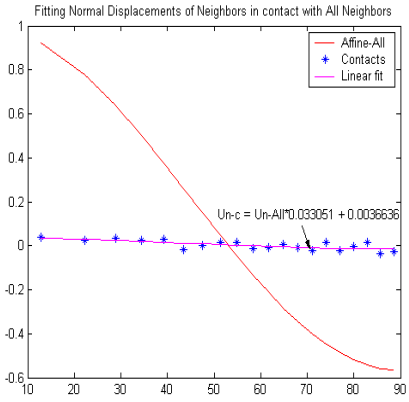

A1 B E

(a) Normal Displacements

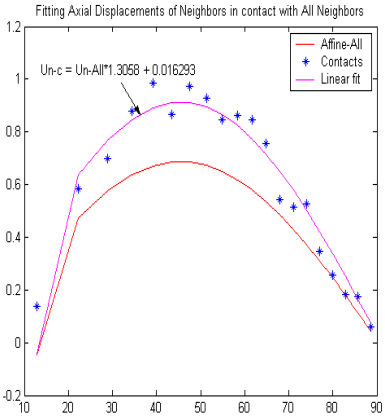

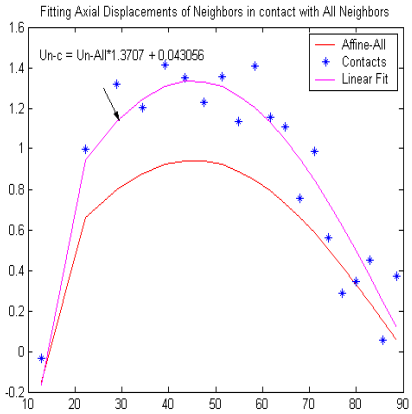

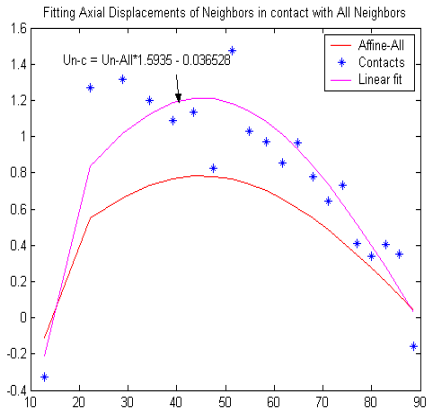

A1 B E

(c) Axial Displacements

Figure 5.2 Fitting displacements of All neighbors with neighbors in contact

Figure 5.2 shows the linear fit of normal and axial displacements of neighbors in contact by the respective displacements of all neighbors at three points of the stress strain curve. The fit works very well for the normal displacements, but gives an approximate least square solution for axial displacements. Similar analysis is done for other points of the stress strain curve of dense sample as well as the loose sample. Table 5.1 and 5.2 lists the coefficients obtained in the linear fit for the dense sample and the loose sample respectively. The relationship between displacement of contacts and displacements of all neighbors can be written in the form U-c = a*U-All + b.

Table 5.1 Coefficients for dense sample

Points on Stress Strain Curve (Figure 3.1)	Normal Displacement		Axial Displacement	
	a	b	a	b
A1	0.30076	0	1.3058	0.0163
A2	0.276	0.05046	1.4076	-0.050
B	0.035446	0.016766	1.3707	0.043
C	0.031462	0.011571	1.446	-0.0425
D	0.015677	0	1.0082	0.3935
E	0.033051	0	1.5935	-0.0365

Table 5.2 Coefficients for loose sample

Points on Stress Strain Curve (Figure 3.1)	Normal Displacement		Axial Displacement	
	a	b	a	b
A1	0.23643	0.0388	1.3213	0.05876
A2	0.12929	0.0199	1.1592	0.18365
B	0.07863	0.0154	1.1964	0.0989
C	0.0123	0	1.6398	0
D	0.0827	0.027	1.2596	0.0967
E	0.01729	0	0.95648	0.44823

6. CONCLUDING REMARKS

The elasto-plastic response of Dirichlet tessellated sample of spherical grains has been investigated in tri-axial loading with the help of discrete element simulations. In spite of the simplicity of the model, it reproduces several aspects of realistic soils. The model has been studied in terms of the micro-mechanical displacements and rearrangements.

The simulations carried out here reflect the inability of affine hypothesis to completely describe micro-mechanical displacements in terms of global parameter like strain. It is verified true for all neighbors, but in micro-mechanical study of granular materials, people are more interested in knowing the behavior of contacts, since grains interact via contacts only. And in our analysis we observe that the affine displacement

field does not give true displacements for grains in contact. Efforts have been made to try to deduce the displacements of grains in contact in terms of the global strain.

The work done here proposes a linear relationship between affine displacement field of all neighbors and the displacement field of neighbors in contact, but the coefficient of linearity varies during loading. The relationship is observed for the loose sample also for the same strain as in dense sample and the coefficient observed are different from dense sample. To study this relationship in detail, it is better to investigate more models with different stiffness to see how it affects the linearity. The results here are mainly for loading. Similar analysis can be done for different loading paths like unloading of the sample to see if the sample behaves in a similar way.

REFERENCES

Bolton M.D. (2000). "The Role of Micro-Mechanics in Soil Mechanics." CUED/D-Soils/TR313

Bagi Katalin. (1996). "Stress and strain in granular assemblies." Mechanics of Materials 22, 165-177

Cambou B., Dubujet P., Emeriault F., Sidoroff F. (1995). "Homogenization for granular materials." Eur. J. Mech., A/Solids, 14, No. 2, 255-276

Cundall P. A., Strack O. D. L. (1979). "A discrete numerical model for granular assemblies." Geotechnique 29, No. 1, 47-65

Kruyt N. P., Rothenburg L. (1996). "Micromechanical Definition of the Strain Tensor for Granular Materials." ASME JOURNAL OF APPLIED MECHANICS, Vol. 118

Kuhn Matthew R. (1999). "Structured deformation in granular materials." Mechanics of Materials 31, 407-429

Nouguier-Lehon C., Cambou B., Vincens E. (2003). « Influence of particle shape and angularity on the behavior of granular materials: a numerical analysis." Int. J. Numer. Anal. Meth. Geomech., 27, 1207-1226

Rothenburg L., Kruyt N. P. (2004) “Critical state and evolution of coordination number in simulated granular materials.” International Journal of Solids and Structures 41, 5763-5774